

THE QUANTITATIVE LIF DETERMINATION OF OH CONCENTRATIONS IN LOW-PRESSURE FLAMES

KATHARINA KOHSE-HÖINGHAUS,* JAY B. JEFFRIES, RICHARD A. COPELAND
GREGORY P. SMITH AND DAVID R. CROSLY

*Molecular Physics Department
SRI International
Menlo Park, California 94025*

Laser-induced fluorescence (LIF) of OH is used to measure spatially resolved temperature and concentration profiles in premixed laminar flames of H_2 burning in mixtures of O_2 and N_2O at 7.2 Torr. Potential sources of error in such measurements are investigated: optical depth; the detector spectral bias, time delay, and sampling gate; and rotational level dependence of the quantum yield for the OH radical. We explicitly demonstrate differences between LIF intensity measurements and the actual OH concentration profiles caused by the temperature dependence of the rotational level populations across the flame front. By varying the proportion of O_2 and N_2O in stoichiometric flames, burnt gas temperatures between 1200 and 2300 K are obtained. Quenching measurements in the burnt gases of these flames show that quenching by atomic hydrogen can be important. In the burnt gases of the H_2/N_2O flame, the quenching does not significantly depend on rotational level for diagnostics with 5% accuracy. However, in the chemically interesting and important flame front, there is a significant variation in the quantum yield with rotational level, and in the flame front of atmospheric pressure flames such quantum yield corrections are likely to be important.

Introduction

The OH molecule as a very important reactive radical in combustion is the focus of many flame investigations using laser-induced fluorescence (LIF).¹ Profiles of [OH] in stable, laminar flames may be compared with computer models of the flame chemistry. Quantitative measurements are needed for this purpose, and it is crucial to determine the temperature in conjunction with the concentrations. Qualitative radical concentration measurements can also be useful; for example, two-dimensional LIF imaging² of relative [OH] in a turbulent flame can provide insight into coupling between the chemistry and the flow.

Several features of the radical's spectroscopic, radiative and collisional behavior demand special care for accurate LIF measurements of [OH]. We describe experiments performed in stable, laminar, low-pressure flames of H_2 burning in O_2 , N_2O , and mixtures of the two oxidants to investigate various influences upon quantitative LIF measurements of temperature and [OH]. Flames at a few Torr offer special advantages: temperature gradients are grad-

ual compared with the laser spatial extent, there is little averaging over temperature-dependent measurement effects, and comparisons with chemical models are more meaningful. Collisional quenching is slow: the excited state lives longer than the laser pulse, and the direct time decay of the fluorescence can be used to study collisional effects.

Temperatures are measured by directly fitting rotational excitation scan spectra. Here, careful attention must be paid to possible systematic errors arising from spectral bandpass, position and width of the detector time gate, optical saturation, and absorption of both laser light and fluorescence. For accurate concentration measurements, the fluorescence quantum yield due to quenching must be known. We find a slight variation of the quantum yield with rotational quantum number N' in the burnt gases, but more than 25% in the zone of increasing temperature. Saturated fluorescence schemes are less sensitive to quenching but introduce new questions about the size of the probed volume.³ For measurements in turbulent flame, one needs to estimate the electronic quenching rate Q (s^{-1}) at different temperatures and mixing ratios. This can be done using information on bimolecular quenching rate coefficients k_Q ($cm^3 s^{-1}$). As anticipated,⁴ the current measurements show little variation in Q with mixing ratio. We also examine the radical profiles and compare them with computer

*On leave from Institut für Physikalische Chemie der Verbrennung, DFVLR, Stuttgart, West Germany.

calculations. Different aspects of the flame chemistry in the H_2/N_2O and H_2/O_2 flames are discussed. H_2 burning in different N_2O/O_2 mixtures furnishes a large range of flame temperatures which permits the study of quenching and rotational level dependent effects.

The results presented in this paper provide a prescription for LIF measurements of OH temperature and concentration in low-pressure flames. Many complications are avoided by using a detection time gate which is short compared with the timescale for collisional quenching and energy transfer of the OH ($A^2\Sigma^+$). Thus, each of the sources of error discussed here must be evaluated for other physical environments, particularly higher pressure. The present results do provide concepts and guidelines for such evaluation.

Experimental Arrangement

The experimental apparatus is discussed in detail elsewhere.⁵ A 6 cm diameter, water-cooled porous plug burner in an evacuated chamber supports flames at 7.2 Torr. The burner can be scanned vertically with an accuracy and reproducibility of 0.1 mm. The laser beam either traverses the burner at the center, with a path length of 3 cm for the fluorescence through the flame or at a position closer to the burner edge, with a 1.25 cm fluorescence path. The collimated laser beam is apertured with 0.38 mm (FWHM) beam size corresponding to a temperature spread of 100 K in the H_2/N_2O flame and 20 K in cooler H_2/O_2 flame. OH and NH are excited in the (O, O) bands of their A-X electronic systems, with light from an excimer-pumped dye laser (15 ns pulse length, $<10 \mu J$ pulse energy).

A two-lens system collects the signal at $f/3$ and focuses it at $f4$ into a 0.3 m monochromator; the 0.5 mm entrance slit parallel to the laser beam, with perpendicular 4 mm stops, defines the probed volume. A 4 mm output slit provides a trapezoidal spectral response with a 20 nm top and 23 nm base. Masking by the burner⁶ of both the laser beam and fluorescence path at low probing height is accounted for in the data analysis. The signal from IP28 photomultiplier is either time resolved with a 100 MHz transient digitizer or integrated with a computer controlled boxcar integrator with variable gates. Two photodiodes monitor the laser intensity, before and after the burner. The ratio of these two signals measures the absorption by the flame OH; typical maxima are 9% for strong lines in the R branch.

Temperature Measurements

Temperatures and species concentrations with precise spatial correlation are crucial to a quanti-

tative comparison between flame measurements and model calculations of the flame chemistry for two reasons. First, temperature is needed to relate number density in a particular rotational level (as measured by fluorescence intensity) to total OH mole fraction. Second, because of the highly nonlinear effect of temperature upon a chemical reaction sequence, an error of 100 to 200 K could mean that chemistry quite different from that calculated, using an imposed experimental temperature profile, is occurring at each point.

Experimental problems can cause significant systematic errors which are not distinguishable from correct values through statistical measures of goodness. We first discuss the method of measurement and second the sources of possible bias.

In our experiments, temperature is measured by rotational excitation scans, using a computer to scan the laser and store the data, which are normalized to laser power. A 10 ns boxcar gate samples the signal soon after the laser pulse, so that little rotational relaxation occurs and fluorescence mainly from the pumped level is measured. (See, e.g., the spectra in Ref. 7.) A series of 18 R_1 , R'_1 and R_2 branch lines with $N'' = 2$ to 15 is used, spanning 0.35 nm which is scanned in 14 min. For $T > 2000$ K, a shorter series of 5 lines with $N'' = 2, 6, 13$ and 15 within a 0.1 nm range scanned in 5 min produces results indistinguishable in quality, each with $<3\%$ 2σ fitting errors (not accuracy). The spectra are fit to two parameters, a temperature and linewidth (constant for all lines), using tabulated line positions⁸ and intensities⁹ which include the effects of a varying electronic transition moment. Direct spectrum fitting has also been done elsewhere;¹⁰ our work on OH, NH, CH and CN is detailed separately.¹¹

Possible error sources in these low-pressure flame experiments include spectral biasing, which has been described in detail for atmospheric pressure flames.¹² If the detection bandpass is centered on an intense region but is not sufficiently wide, fluorescence from high N' will be detected less efficiently, and produce temperatures which appear lower than actual. At higher pressure, the lack of rotational thermalization before quenching makes this a problem. At low pressure with a short gate no relaxation occurs and the problem is even more acute. The spectral response used here, which includes the entire R and Q branches as well as P-branches up to $N' = 30$, is fully adequate for pumping $v' = 0$ in OH.

The second concern is the choice of gate delay time. Higher N' have longer radiative lifetimes and are collisionally removed more slowly. Consequently, moving the gate to longer delays will increase the relative amount of fluorescence from higher N' , and the apparent temperature will become higher. At 7 Torr, a 100 ns lifetime and 2300 K, the systematic error ΔT increased smoothly from

80 K at 50 ns delay to 240 K at 250 ns; integrating over the entire decay yielded $\Delta T = 100$ K. When a prompt gate is used, as in many of these experiments, one must consider the relationship between measured initial amplitude and excited state population by using the appropriate radiative decay rates. This initial amplitude is lower for those high N' levels which have a longer radiative lifetime.

The optical depth of the flame must be considered quantitatively, because 10% absorption can produce errors of 100 K or more. The highly populated lower N'' in the cooler flame boundary (which also have larger oscillator strengths) absorb more and the lines appear weaker than they should, yielding too high an apparent temperature. Absorption of the laser beam as it traverses the burner, and of the fluorescence as it propagates outward through the flame, must both be considered. In our flames, neglect of the optical depth leads to $\Delta T \sim 80$ K at 2000 K, but <25 K at 1200 K where there is less of a temperature gradient at the flame boundary and a smaller variation in the oscillator strength of the populated levels.

For most of our experiments, the path length through the flame is 5 cm for the laser beam and 1.25 cm for the fluorescence. The laser is absorbed only in the R-branch. The prompt gate ensures that most observed fluorescence originates from, and is reabsorbed by, the same initially excited levels. The fluorescence is reabsorbed in all three rotational branches each of which have different line strengths. For the chosen path lengths it turns out that absorption of the laser in the R-branch with its longer path length is just equivalent to absorption of the fluorescence in all three P-, Q-, R-branches over its shorter path. Thus, calculations of the actual optical depths show that normalization of the LIF signal by the post-flame photodiode signal properly corrects for absorption of both the laser and fluorescence. Such computations must be made for each experimental beam path setup.¹¹ Temperatures and radical concentration profiles measured at the center of the burner agreed with those taken at the position closer to the edge, ensuring that the flame is sufficiently flat that the latter are meaningful.

Figure 1 shows the temperature profiles obtained for the H_2/N_2O and H_2/O_2 flames at 7.2 Torr. Measurements in the O_2 -based flame are made to extremely low temperatures, <400 K. In the H_2/N_2O flame, LIF excitation scan rotational temperatures in NH, which are free from spectral and absorption biasing, agree with the OH temperatures to within error bars.

Quenching by Flame Gases

Measurements in flames at atmospheric pressure, particularly in time-varying systems where two-di-

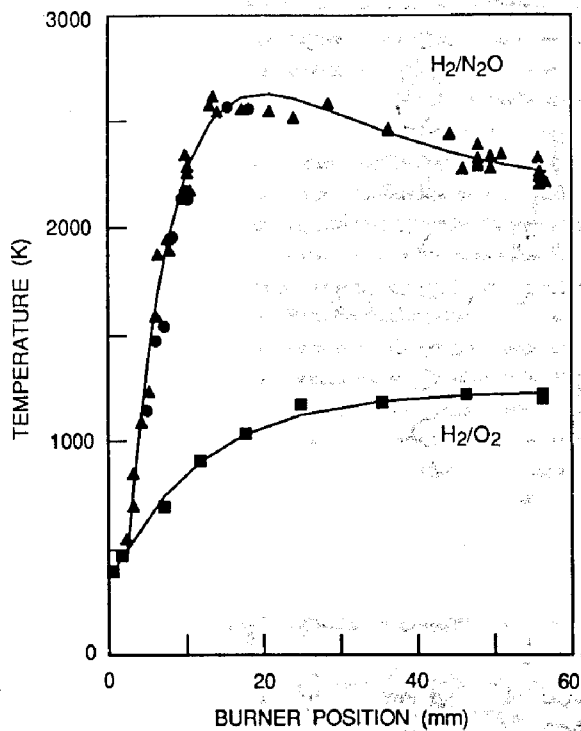


FIG. 1. Rotational excitation scan measurements of temperature in stoichiometric H_2/N_2O (boxes) and H_2/O_2 (triangles) flames at 7.2 Torr versus height above the burner. NH rotational temperatures in the H_2/N_2O flame (circles) are shown for comparison. The lines are (fully empirical) double-exponential fits to the data.

mensional images are desired, require knowledge of the quenching rate Q for excited OH. This determines the fluorescence quantum yield, which relates measured LIF intensities to ground state radical concentrations. Previous measurements at room¹³ and elevated^{14,15} temperatures (240 to 1400 K) show several features of OH quenching important for LIF diagnostics: σ_Q varies with collider species, with N' and with T. The N' dependence is important as excited OH does not rotationally thermalize before quenching occurs. Reference 4 discusses how to use previously determined σ_Q for individual colliders to calculate Q for various flames and temperatures, with an estimated accuracy of 30% if the temperature and the flame gas composition are known. One potential difficulty with this approach is that quenching due to radicals (H, O, OH itself) is not known.

Here fluorescence decay rates are measured in a stoichiometric H_2/N_2O flame. Quenching in the pure H_2/O_2 flame usually proceeds too rapidly for our digitizer bandwidth, although one measurement in the burnt gases at 1200 K is made (see below). The fluorescence decay traces are fitted to a single exponential from an amplitude of 90% to 10% of maximum. The radiative rate (also a function of N')^{9,16} is then subtracted to determine Q , which is then

divided by the density to obtain k_Q . Plots of k_Q vs. burner position for three separately pumped N' are shown in Fig. 2. The numerical results show a small decrease with N' : at 7.2 Torr in the burnt gases, $k_Q = 3.14, 3.08$ and $3.00 \times 10^{-10} \text{ cm}^3 \text{ s}^{-1}$ for $N' = 3, 8$ and 16 , respectively, which is interesting from the viewpoint of fundamental collision dynamics but of little significance for diagnostic purposes. In flames at higher pressure where quenching dominates the removal of the excited state, the rotational dependent quantum yield would cause a 60–80 K error in the temperature.

Closer to the burner surface, however, a marked variation in the k_Q is observed with N' which reflects changes in the N' dependence with temperature and/or chemical composition. Therefore, in this important flame zone, the quantum yield may not be regarded as constant with N' . From the data in Fig. 2, the quantum yield varies by 25% between $N' = 3$ and $N' = 8$ in the flame front. In these low-pressure flames, the use of prompt sampling of the LIF with a time gate short compared

to the fluorescence lifetime avoids corrections to the temperature and concentration profiles for these rotational level dependent quantum yields; however, in the flame front of an atmospheric pressure flame, such quantum yield corrections may be important.

Knowledge of the dependence of k_Q in the burnt gases on the mixing ratio can help estimate OH concentrations in turbulent systems, especially where two-dimensional imaging is used. In such cases the collision environment is not well known. Figure 3 shows a small variation of k_Q with equivalence ratio in the burnt gases, where the predominant quencher H_2O is present in similar amounts. For such stable flames, the usual practice of assuming constant k_Q would be accurate to within 30%. This conclusion must be used with caution; it is unlikely to generally apply to every combustion situation.

Concentration Profiles

Figure 4 shows concentration profiles of OH as a function of height above the burner for the stoichiometric $\text{H}_2/\text{N}_2\text{O}$ flame. The conversion of fluorescence profiles from different excited rotational levels to a profile of total OH number density illustrates the importance of accurate temperature measurements. For these measurements, a narrow gate with a 10 ns delay after the laser pulse is used so that quantum yield corrections are unnecessary. The laser intensities are converted to OH mole fractions using the empirical temperature profiles.

The top panel of Fig. 4 shows the original intensities for $N'' = 2, 7$ and 15 scaled to fit in one graph. The large differences in temperature-dependent fractional populations $f(N'')$ for the three levels

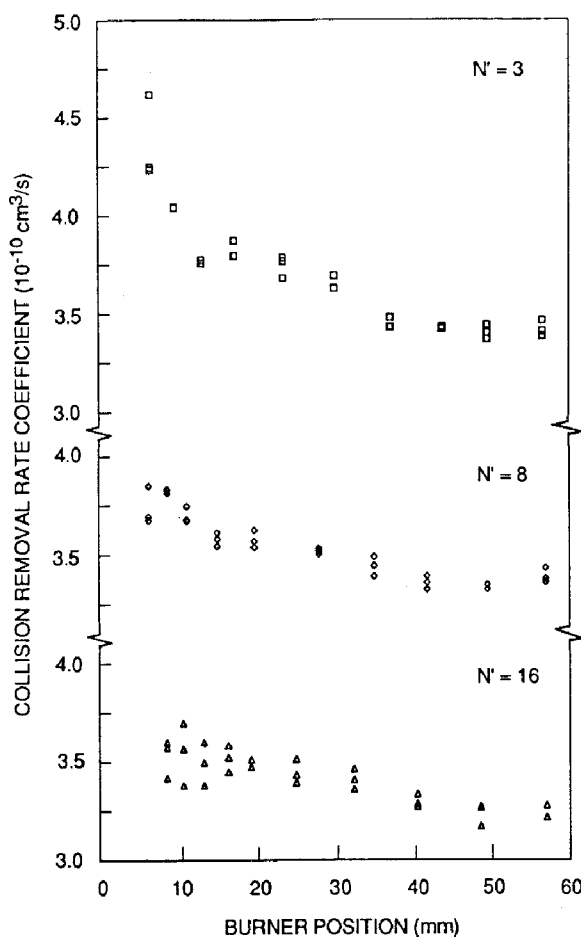


FIG. 2. Collisional removal rate coefficient for OH with $N' = 3, 8$, and 16 versus height above the burner measured in the stoichiometric $\text{H}_2/\text{N}_2\text{O}$ flame that has the temperature profile of Fig. 1.

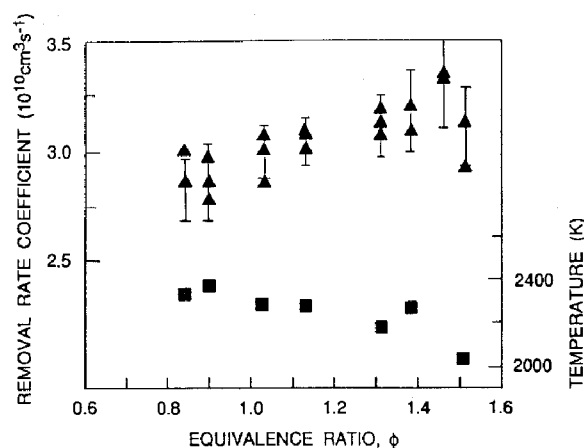


FIG. 3. Collisional removal rate coefficient (triangles) for OH, $N' = 8$, versus equivalence ratio for a $\text{H}_2/\text{N}_2\text{O}$ flame measured in the burnt gases, 50 mm above the burner; error bars are 2σ . The (squares) give the measured temperature at the same points in the flame.

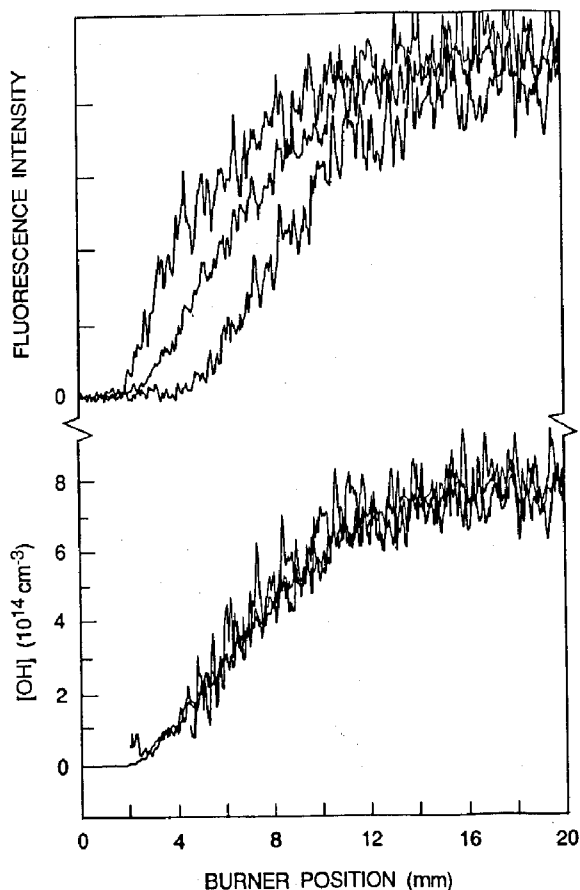


FIG. 4. Upper panel: fluorescence intensity of OH LIF versus height above the burner for a 7.2 Torr stoichiometric $\text{H}_2/\text{N}_2\text{O}$ flame. The three different traces are for $N'' = 2, 7,$ and 15 ; these are scaled to the same value at 20 mm burner height. Lower panel: OH concentrations derived from these same three intensity measurements and the temperature profile of Fig. 1. Note the overlap to within noise. The relationship between the traces in the upper and lower panels involve only thermal population fractions for the N'' , the level degeneracies, and the appropriate oscillator strengths. The absolute scale is determined by an absorption measurement at burner height 50 mm in the burnt gas region of the flame.

are especially pronounced in the flame front region. The lower panel shows the consistent concentration profiles resulting from each of these intensity profiles, when different amplifier gain, oscillator strengths and Boltzmann fractions are considered. They have been placed on an absolute basis by the absorption measurements in the burnt gases. The concentration profiles determined from $N'' = 7$ and 15 terminate near 4 mm; here the temperature is so low that these $f(N'')$ are $<1\%$ of their maximum values. An intermediate level like $N'' = 7$ is the best overall choice of level to monitor, because $f(N'' = 7)$ varies the least with temperature over

this range. One cannot, however, neglect the correction for changing Boltzmann fraction: the upper and lower trace for $N'' = 7$ in Fig. 4 are different in the flame front. $N'' = 2$ yields better signal to noise ratios near the burner at low temperature.

Flame Chemistry Calculations

Computer modelling of our low-pressure flames is performed to determine major stable and radical species concentrations necessary to interpret the quenching measurements in the mixed oxidant flames (and not for a comprehensive comparison between model and experiment). The reliability of the calculations for this purpose is judged by comparison with OH profiles. We use the Sandia code PREFLAME¹² which incorporates the detailed chemistry package CHEMKIN.¹⁸ The measured temperature profiles are imposed as input with $T = 370$ K at the burner surface. The chemical reaction mechanism¹⁹ is adapted from Coffe.²⁰ The H_2/O_2 rate constants are those of Warnatz,²¹ and include all the potential recombination reactions. The N_2O rate constants are largely those recommended by Hanson and Salimian,²² although more recent values²³ are used for the key $\text{H} + \text{N}_2\text{O}$ reactions which produce OH or NH. Coefficients for the reactions of NH with radicals that control the decay of the NH profile are estimates, including our own guess of $5 \times 10^{-12} \text{ cm}^3 \text{ s}^{-1}$ for NH reacting with either NH or OH. We omit the species H_2O_2 , HNO, and NH_2 after the model calculations show they lack chemical significance for our purposes and under our conditions.

The comparison between calculated and measured radical profiles for the stoichiometric $\text{H}_2/\text{N}_2\text{O}$ flame is illustrated in Fig. 5. Computed and measured [OH] profiles agree in shape and absolute values to within the 30% ($1 - \sigma$) error estimated for the absolute scale determined from the absorption measurement. The [NH] profile gives only relative concentration. The stoichiometric $\text{H}_2/\text{N}_2\text{O}$ flame burns hot even at low pressure because the bimolecular chain steps proceed to the final products. The magnitude and position of the NH profile are determined by the balance between the $\text{H} + \text{N}_2\text{O}$ reaction, one channel of which forms the radical, and destruction reactions with various other radicals, especially H. These latter rate constants are not known experimentally but are estimated, although with considerable uncertainty. The OH rise is also controlled primarily by $\text{H} + \text{N}_2\text{O}$, and the good fit confirms this portion of the model. At burner heights above the [NH] maximum, the model disagrees with the experimental results indicating loss rates that are too slow. Future experiments including absolute [NH] determinations should clarify these

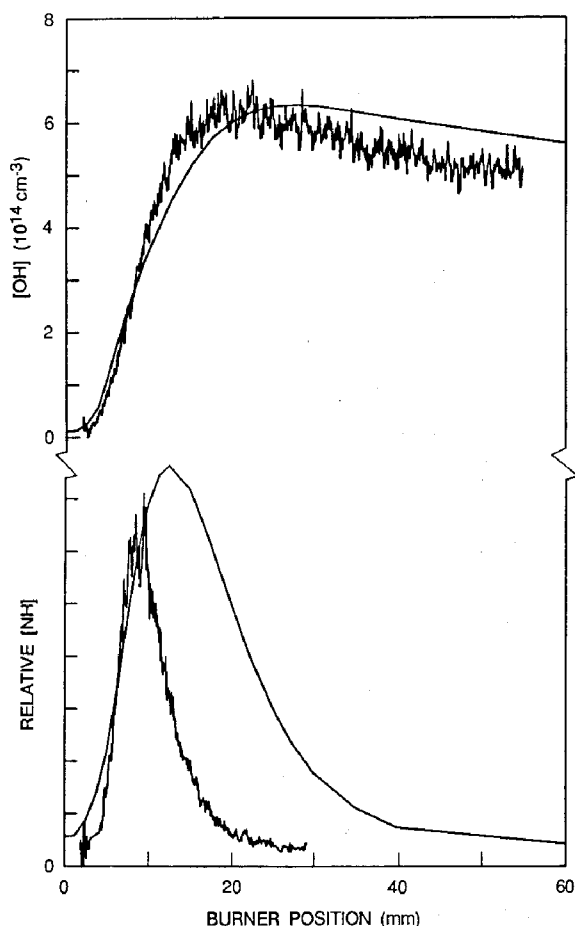


FIG. 5. Upper panel: OH concentration versus height above the burner. The smooth curve gives the scaled results of the model calculation which is multiplied by 1.3 to scale both curves to a common maximum. Experimental and calculated [OH] agree within the estimated 30% error limit on the absolute scale. The lower panel displays the relative [NH] measurement and model for the same flame.

key unknown rate constants and the $H + N_2O$ branching ratio.

By contrast the H_2/O_2 flame burns quite cold at low pressure despite the large enthalpy available. The burnt gas temperature in our burner (see Fig. 1b) is 1200 K, which is a difference from the high $T_{adiabatic}$ that has been noted earlier.²⁴ The final energy release steps are pressure-dependent recombination reactions which proceed very slowly. Thus the chain branching reactions yield very high burnt gas radical concentrations; H and OH remain un-recombined. These radicals, particularly the light H atoms, also diffuse back into the unburnt gases, yielding high radical concentrations at very low temperatures near the burner; recall that there is sufficient OH for temperature measurements at 390 K, 1 mm above the burner. The OH in fact has two density maxima, as previously observed.^{24,25} The

first, near the burner surface, diminishes as the total density decreases with increasing T , and the second grows in as the OH mole fraction increases with reactions in the main flame zone. The model calculation matches this rise well, although in this case, our experimental data are subject to greater uncertainty: due to fast quenching in the flame front zone, our 10 ns gate is not short in comparison to the collisional decay time.

The large difference in burnt gas temperatures of the two flames suggests the use of H_2 burning in O_2/N_2O mixtures to obtain a temperature range in a relatively simple gas environment. In the following section we describe the use of such mixed oxidant flames to investigate the possible temperature dependence of OH quenching due to H_2O . For this purpose model calculations of concentrations of important species are performed for oxidizer ratios of $2N_2O/O_2 = 0.66, 1.0, 1.33, 1.67,$ and 2.0 using measured burnt gas temperatures and imposed temperature profiles similar in shape to that of the H_2/N_2O flame (see Fig. 6). The similar flame front position of all these 7 Torr stoichiometric flames and the dominant initial role of the N_2O chemistry justify this choice. The calculated burnt gas composition is relatively insensitive to such details.

Quenching in Mixed Oxidant Flames

For the investigation of the quenching of OH at different temperatures, the temperature in the

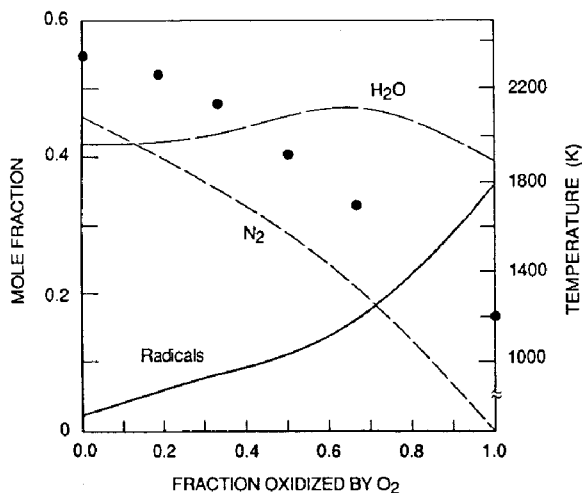


FIG. 6. The solid and dashed lines are model calculation results for mole fractions of N_2 , H_2O , and radicals (mostly atomic hydrogen) at a burner height of 5 cm for stoichiometric $H_2/O_2/N_2O$ flames at 7.2 Torr versus the fraction of fuel oxidized by O_2 . Measured temperatures in the burnt gases at the same burner height are plotted as points. As O_2 replaces N_2O the flame burns substantially cooler and the H atom concentration increases dramatically.

$\text{H}_2/\text{O}_2/\text{N}_2\text{O}$ flames is varied from 1200 K (pure O_2 oxidant) to 2300 K (pure N_2O). The burnt gas composition varies at the same time, so interpretation of the results is not unambiguous. However, interesting conclusions concerning OH quenching can be drawn: the N' dependence of the quenching rate for H_2O collider decreases between 300 and 2300 K, H atoms are an important quencher for OH in a low-pressure H_2/O_2 flame, and the quenching cross section for H_2O decreases no more than 20% between 1200 and 2300 K.

Removal rate coefficients k_Q at different temperatures, exciting the three levels $N' = 3, 8$ and 16 are given in Fig. 7. For the pure H_2/O_2 flame at 1200 K, only a single and less precise value for $N' = 7$ was determined. k_Q decreases at higher temperature even though the relative collisional velocity increases, which indicates a decreasing σ_Q and/or a composition dependence. A small but real N' dependence at the lower temperature disappears at the highest temperatures.

In the burnt gases of the $\text{H}_2/\text{N}_2\text{O}$ flame at 2320 K, Fig. 6 shows that the major species are N_2 and H_2O . N_2 quenches OH poorly,¹⁴ and we estimate that H_2O is responsible for >80% of the OH quenching. The data in Fig. 7 near 2300 K show less than a 5% N' dependence for $3 < N' < 16$, whereas at room temperature, $\sigma_Q(\text{H}_2\text{O})$ decreases¹³ by $\sim 15\%$ between $N' = 3$ and 7. Thus, there is a decrease in the N' dependence of the OH quenching by H_2O with increasing temperature. The decrease shown in Fig. 7 for the N' dependence of k_Q with increasing temperature between 1200 and 2300 K may reflect this temperature dependence for the H_2O collider, or it may only reflect a substantially larger N' dependence for the quenching of OH by other colliders present in the flames at lower temperature.

Using the model calculations discussed above, we find atomic hydrogen to be the only species of significant concentration in the burnt gases of the H_2/O_2 flame for which a quenching cross section at 1200 K is not known. Using the model calculations for $[\text{H}]$ and $[\text{H}_2\text{O}]$ and the measurement of Q in Fig. 7 at 1200 K as well as the cross sections of Ref. 14, we estimate $\sigma_Q(\text{H}) = 15 \pm 5 \text{ \AA}^2$; this is consistent with the $\sigma_Q(\text{H}) = 22 \text{ \AA}^2$ reported²⁶ at 300 K. Thus, even at 35 mm above the flame front in this 7.2 Torr H_2/O_2 flame, collisions of OH with H atoms account for >50% of the quenching.

The average k_Q in Fig. 7 decreases 30% as T increases from 1200 to 2300 K for two reasons. First, $\sigma_Q(\text{H}_2\text{O})$ decreases with increasing temperature,¹⁴ from 70 \AA^2 at 300 K to $\sim 26 \text{ \AA}^2$ at 1200 K for $N' = 7$. If the mechanism for the quenching is dominated by long-range attractive forces, at higher temperature the decrease should continue but at a lesser rate, as observed¹⁵ for $\sigma_Q(\text{NH}_3)$ between 300–1400 K. Second, the large decrease in the radical

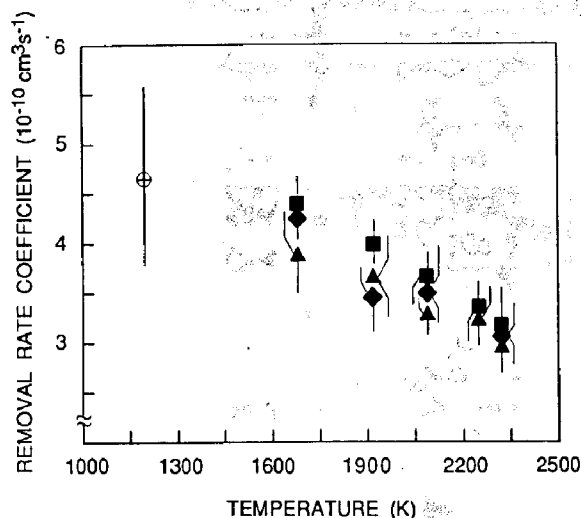


FIG. 7. Quenching rate coefficients for OH $N' = 3$ (boxes), $N' = 8$ (diamonds) and $N' = 16$ (triangles) versus temperature in stoichiometric H_2 flames at 7.2 Torr with mixtures of O_2 and N_2O oxidant. The measurement at 1200 K (circle) is for $N' = 7$. Error bars are 2σ .

concentration, mostly hydrogen atoms, as N_2O replaces O_2 (see Fig. 6), eliminates quenching by H in the higher temperature flames. We can describe the results for average k_Q in Fig. 7 in two limits. The first is $\sigma_Q(\text{H}) = 10 \text{ \AA}^2$ constant with temperature and $\sigma_Q(\text{H}_2\text{O})$ decreasing from 50 \AA^2 at 1200 K to 28 \AA^2 at 2300 K. This is too high a $\sigma_Q(\text{H}_2\text{O})$ at 1200 K. The second limit is $\sigma_Q(\text{H}) = 15 \text{ \AA}^2$ and $\sigma_Q(\text{H}_2\text{O}) = 25 \text{ \AA}^2$, respectively, each constant with temperature. However our physical picture¹³⁻¹⁵ of the quenching mechanism indicates σ_Q should decrease over this range. We conclude that there is likely a very slight decrease in both σ_Q over this temperature range, and that quenching by H atoms contributes significantly at the lower temperatures.

Conclusion

This work provides concepts to perform accurate temperature and radical concentration measurements. Several aspects of fundamental interest are emphasized. Quantum yield corrections, which we avoid by fast gating in our low-pressure flames, are likely to affect time-integrated measurements at atmospheric pressures. OH removal in the burnt gases varies only slightly with mixing ratio in the example given, an encouraging result with respect to imaging studies. We observe a significant variation of the OH total removal rate with rotational level N' throughout the flame front. Quenching is negligibly N' -dependent in the burnt gases of our $\text{H}_2/\text{N}_2\text{O}$ flame (with H_2O as dominant quencher) at 2300 K, a considerable decrease of this effect in comparison

to room temperature. These data contribute valuable information with respect to the collision dynamics. In our H_2/O_2 flame at 1200 K, quenching by H atoms could be estimated, providing a first limit of the potential importance of quenching by radicals at flame temperatures.

Acknowledgment

We thank Karen Rensberger and Michael Wise for help during the development of the experimental method for the measurement of NH profiles and temperatures, and Mark Dyer for participation in design and construction of the burner system. This work was supported by the U.S. Department of Energy, Division of Basic Energy Sciences.

REFERENCES

1. CROSLLEY, D. R. and SMITH, G. P.: *Opt. Engr.* 22, 545 (1983); BECHTEL, J. H., DASCH, C. J. and TEETS, R.: in *Laser Applications* (Erf, R. K. and READY, J. F., Eds.) Academic Press, New York, 1983; LUCHT, R. P.: in *Laser Spectroscopy and Its Applications* (RADZIEMSKI, L. J., SOLARZ, R. W., and PAISNER, J. A. Eds.) Marcel Dekker, New York, 1986; CROSLLEY, D. R.: *High Temp. Mat. Proc.* 7, 41 (1986).
2. DYER, M. J. and CROSLLEY, D. R.: *Opt. Lett.* 7, 382 (1982); HANSON, R. K.: *Twenty-First Symposium (International) on Combustion*, p. 1677. The Combustion Institute, 1988.
3. KOHSE-HÖINGHAUS, K., HEIDENREICH, R., and JUST, TH.: *Twentieth Symposium (International) on Combustion*, p. 1177. The Combustion Institute, 1984; KOHSE-HÖINGHAUS, K., KOCZAR, and P., JUST, TH.: *Twenty-First Symposium (International) on Combustion*, p. 1719. The Combustion Institute, 1988; SALMON, J. T., LAURENDEAU, N. M.: *Appl. Opt.* 24, 1313 (1985).
4. GARLAND, N. L. and CROSLLEY, D. R.: *Twenty-First Symposium (International) on Combustion*, p. 1693. The Combustion Institute, 1988.
5. RENSBERGER, K. J., DYER, M. J. and COPELAND, R. A.: *Appl. Opt.* 27, 3679 (1988).
6. ANDERSON, W. R., DECKER, L. J., and KOTLAR, A. J.: *Comb. Flame* 48, 179 (1982).
7. LUCHT, R. P., SWEENEY, D. W., and LAURENDEAU, N. M.: *Appl. Opt.* 25, 4086 (1986).
8. DIEKE, G. H. and CROSSWHITE, H. M.: *J. Quant. Spect. Rad. Trans.* 2, 97 (1962).
9. CROSLLEY, D. R. and LENGEL, R. K.: *J. Quant. Spect. Rad. Trans.* 15, 579, (1975); CHIDSEY, I. L. and CROSLLEY, D. R.: *J. Quant. Spect. Rad. Trans.* 23, 187 (1980).
10. ANDERSON, W. R., DECKER, L. J., and KOTLAR, A. J.: *Comb. Flame* 48, 163, (1982).
11. RENSBERGER, K. J., JEFFRIES, J. B., COPELAND, R. A., KOHSE-HÖINGHAUS, K., WISE, M. L., and CROSLLEY, D. R.: to be published.
12. SMITH, G. P. and CROSLLEY, D. R.: *Eighteenth Symposium (International) on Combustion*, p. 1511. The Combustion Institute, 1981; CROSLLEY, D. R. and SMITH, G. P.: *Comb. Flame* 44, 27 (1982).
13. COPELAND, R. A., DYER, M. J. and CROSLLEY, D. R.: *J. Chem. Phys.* 82, 4022 (1985); COPELAND, R. A. and CROSLLEY, D. R.: *J. Chem. Phys.* 84, 3099 (1986).
14. FAIRCHILD, P. W., SMITH, G. P. and CROSLLEY, D. R.: *J. Chem. Phys.* 79, 1795 (1983); SMITH, G. P. and CROSLLEY, D. R.: *J. Chem. Phys.* 85, 1898 (1986).
15. JEFFRIES, J. B., COPELAND, R. A. and CROSLLEY, D. R.: *J. Chem. Phys.* 85, 1898 (1986).
16. BRZOWSKI, J., ERMAN, P., and LYRA, M.: *Phys. Scr.* 17, 507 (1978); BAUSCHLICHER, JR., C. W. and LANGHOFF, S. R.: *J. Chem. Phys.* 87, 4665 (1987).
17. KEE, R. A., GRGAR, J. F., SMOOKE, M. D., and MILLER, J. A.: *Sandia National Laboratory Report SAND85-8240*, 1985.
18. KEE, R. A., MILLER, J. A., and JEFFERSON, T. H.: *Sandia National Laboratory Report, SAND80-8003*, 1980.
19. SMITH, G. P., "Chemical Mechanism for Modeling Low Pressure $H_2-N_2O-O_2$ Flames," *SRI Report MP 88-006*, January 1988.
20. COFFEE, T. P.: *Comb. Flame* 65, 53 (86).
21. WARNATZ, J.: in *Combustion Chemistry* (W. C. GARDINER JR., Ed.) Chap. 5, Springer Verlag, New York, 1984.
22. HANSON, R. K. and SALIMIAN, S. in *Combustion Chemistry* (W. C. GARDINER JR., Ed.) Chap. 6, Springer Verlag, New York, 1984.
23. MARSHALL, P., FONTIJN, A., and MELIUS, C. F.: *J. Chem. Phys.* 86, 5540 (1987).
24. EBERIUS, K. H., HOYERMANN, K. and WAGNER, H. GG.: *Thirteenth Symposium (International) on Combustion*, p. 713. The Combustion Institute, 1971.
25. SALMON, J. T. and LAURENDEAU, N. M.: *Appl. Opt.* 25, 2881 (1987).
26. BECKER, K. H., HAAKS, D. and TATARCZYK, T.: *Chem. Phys. Lett.* 25, 564 (1974).

COMMENTS

N. J. Brown, Lawrence Berkeley Laboratory, USA. This is an extremely fine piece of research. The H atom quenching cross section is quite large. This may be understood by considering that the O atom of OH sets at the center-of-mass while the H atom rotates rapidly around and interacts impulsively with the incoming H atom. Your H atom cross section was determined subtractively, what do you estimate the errors to be?

Author's Reply. Such a dynamical picture may well be appropriate for quenching by many colliders, because there are many molecules which quench OH as efficiently as do H atoms (although they do have larger gas kinetic cross sections). The cross section was determined subtractively, that is, one measurement with all other cross sections assumed known. The quoted 30% error includes estimates of uncertainty in the measurement, the known cross sections, and particularly the H atom concentration as predicted from our flame chemistry model.

D. A. Greenhalgl, Harwell Laboratories, England. Why did you choose N_2O as an oxidant rather than $N_2:O_2$ mixtures?

Author's Reply. The idea of using the mixtures of O_2 and N_2O oxidant was to vary the temperature between the limits of 1200 K and 2300 K obtainable in our system. Using N_2/O_2 mixtures would only lower the temperature from the 1200 K value obtained in pure O_2 .

S. Koda, Tokyo Univ., Japan. The quenching rate constant of OH by H atoms may be dependent on π^+ , π^- states as well as spin substates. Have you ever checked such a possibility?

Isn't it possible to determine the temperature on the basis of Doppler profile of OH excitation spectrum?

Author's Reply. In the excited state the parities alternate with each rotational level, so any such effects would be indistinguishable. The quenching of different spin substates (F_1 and F_2 levels) was measured at room temperature (Ref. 21 of the paper). It was the same, as one might expect for collision dynamics governed by the mechanical rotation.

The Doppler profile can yield temperature information, given a sufficiently narrow laser, but it is not as accurate as excitation scans. In any event, our laser has too broad a bandwidth (0.3 cm^{-1}) to provide good Doppler width measurements. How-

ever, we do observe a systematic increase in the width with increasing temperature.

K. Schofield, Univ. of California, USA. There are potential risks in burning stoichiometric flames in that this is a singularity in which only H_2O and any inert diluent are the major product species. The nature of the calibration of flows is such that the resulting flame inevitably has to be slightly fuel rich or lean due to inaccuracies. This can introduce an additional uncertainty in H_2 or O_2 concentrations, respectively. Have you considered trying to analyze the data with slightly rich or lean compositions?

Also, you do have uncertainties in flame temperatures and composition and so various adjustable parameters with which to model the quenching rates. Is it possible that these might alleviate your need to invoke H-atom quenching which has to be regarded by some as speculative at present due to these possible variations and errors.

Author's Reply. Inaccuracies in the exact stoichiometry introduce little uncertainty in the burnt gas species concentrations. For example, calculated mole fractions of major species vary by .01 or less when the hydrogen-oxygen equivalence ratio is raised from 1.0 to 1.05. As to the importance of the H atom quenching, the estimated uncertainty in our cross section includes possible effects of temperature, composition, and other quenching rate constant errors. Since the quenching rate constants for the other major species are known independently, we can determine the only unknown, the H atom quenching rate constant. The water accounts for 36% of the quenching, unburned O_2 and H_2 10%, O atoms and OH are estimated (with large 25 \AA^2 cross sections) to contribute 3% leaving 51% of the quenching due to H atoms. The results clearly indicate the significance of hydrogen atom quenching in these flames.

T. Just, DFVLR, Fed. Rep. of Germany. Your measurements on collisional energy transfer from the excited OH state seem to show that besides the obvious shift to neighboring rotational states there exists a considerable contribution of transfer of larger amounts of energy resulting in the population of other than the aforementioned states.

Do you have suggestions or indications from your experiments, which other states were populated and what are the rate coefficients?

Author's Reply. Rotationally resolved fluorescence spectra¹ show that transfer has occurred not

only to neighboring levels ($\Delta J = \pm 1$) but there is some population in levels with $|\Delta J| \geq 2$. About 35% of the OH remains in the excited level and the remainder is distributed among both higher and lower N' , so that the averaged cross section represents that of the initially excited level.

Where the energy goes in the quenching process itself is not known. Because the OH is in $v' = 0$ of $A^2\Sigma^+$, the energy must go into internal levels of the OH, internal levels of the collider, and/or translational energy of the pair. In our measurements, all we observe is the disappearance of the excited OH, so we cannot tell which final states are populated. Some information is available from a different experiment.² In a low pressure discharge cell, where the dominant collider was H_2O , one laser pumped $v' = 0$ of OH $A^2\Sigma^+$. A second laser, time-delayed from the first, probed the $v'' = 1, 2$ and 4 vibrational levels in ground state OH. Each was collisionally populated after some time delay, and

not as an immediate product of the quenching. Thus, for at least that collider, some of the energy goes into high vibrational levels of the OH, and cascades down through lower levels. Although the exact branching ratios are undetermined, it is clear that the OH does not go predominantly to $v'' = 0$ as would be predicted from a Franck-Condon picture of quenching.

REFERENCES

1. J. B. JEFFRIES, K. H. KOHSE-HÖINGHAUS, G. P. SMITH, R. A. COPELAND AND D. R. CROSLY, *Chem. Phys. Lett.*, in press, 1988.
2. D. R. CROSLY, R. A. COPELAND AND J. B. JEFFRIES, 'State-Specific Energy Transfer in Diatomic Radicals,' SRI Report No. MP88-205, August 1988.